NUMERICAL STUDY OF TAYLOR BUBBLE BREAKUP BY PLACING OBSTACLE AT THE T-JUNCTION BIFURCATION

Sangram Kumar Samal

Department of Mechanical Engineering

National Institute of Technology Rourkela

Email: sangramkumar.samal@gmail.com

Manoj Kumar Moharana

Department of Mechanical Engineering

National Institute of Technology Rourkela

Email: mkmoharana@gmail.com

ABSTRACT

A two-dimensional numerical study of Taylor bubble breakup is carried out, where Taylor bubble flows in a horizontal T-section microchannel with T-junction bifurcation. The numerical simulation is performed using the Volume-of-Fluid multiphase model using commercially available ANSYS Fluent®. The Taylor bubble is formed at the upstream T-junction where air and water enters through two inlets perpendicular to each other. At the end of the channel, the Taylor bubble breaks up symmetrically into two equal size at the bifurcated T-junction. For controlled breakup of the Taylor bubble into two unequal lengths, an obstacle is positioned at the T-junction bifurcation to which the Taylor bubble strikes. The bubble breakup will be symmetrical, asymmetrical or no breakup depending on the position and height of the obstacle. In this work, the obstacle position varied from X = 0 to 0.1 mm, where X is the distance from the center of T-junction bifurcation to the obstacle, and height is varied from Y = 0.05 to 0.2 mm. The symmetrical breakup of the bubble occurs when there is no obstacle, due to the equally distributed flow rate. The symmetrical breakup process also occurs when the obstacle positioned at the center of the T-junction

bifurcation irrespective of the height of the obstacle. When the obstacle position shifted to one side of the T-junction bifurcation, asymmetrical bubble breakup takes place. This occurs because, as the obstacle shifted to one side (say right side) of the T-junction bifurcation, the right side opening decreases and the resistance to flow increases. So, the bubble breaks into two unequal lengths. The length of the bifurcated bubble is higher along the outlet path opposite to that of the obstacle position. When the opening on one side of the obstacle decreases beyond some threshold value, the bubble will not be able to pass through this opening and will result in no bubble breakup.

Keywords: Taylor bubble, microchannel, T-junction bifurcation, bubble breakup, two phase.

1. INTRODUCTION

Now-a-days two-phase flow in microchannel has a broad range of applications in biomedicine, microfiltration, microscale heat transfer enhancement, micro-reactor, chemical synthesis, lab-on-chip technology, etc. When two different immiscible fluids flow inside a microchannel, various flow regimes are created. These flow regimes are bubble flow, churn flow, annular flow, and Taylor bubble flow, etc. From these different types of flow, Taylor bubble flow pattern mostly used. Taylor bubble flow is a gas-liquid flow regime, which consists of elongated bubbles separated by liquid slugs. The bubble generation and breakup are some operations that are obtained in droplet/bubble based microfluidic system. The breakup of the bubble/droplet can be obtained in so many ways such as varying the geometry of the channel, by using some heating arrangements, by placing an obstacle in the channel, etc. The bubble/droplet breakup can be of three types; symmetrical breakup, asymmetrical breakup and no breakup. Due to various applications of this droplet/bubble based microfluidic system in many industries, numerous investigations have been conducted to study these microfluidic systems.

In recent years, research on bubble/droplet-based microfluidic systems gained momentum. Thorsen *et al.* [1] experimentally studied the dynamic pattern formation in a vesicle-generating microfluidic device. Stone *et al.* [2] gives the overview of flows in microfluidic devices and focused on different parameters like mixing, dispersion, bubble generation, transportation, controllability, and reproducibility, etc. Tice *et al.* [3] described some experimental conditions required for the formation of nano-liter sized droplets of aqueous reagents which flows in an immiscible carrier fluid within a microchannel. Link *et al.* [4] proposed two methods for generating unequal sized droplets in a microfluidic device. In one method, they used T-junction with the unequal branch. In second method, obstacle is employed in the straight channel

for the droplet breakup process. Garstecki *et al.* [5] studied the formation and breakup of bubbles and droplets in a microfluidic T-junction. Jousse *et al.* [6] studied both experimentally and numerically the bifurcation of droplet flows within capillaries. Ting *et al.* [7] studied both experimentally and numerically the droplet breakup process by using thermally induced surface tension gradient in a microchannel. A T-junction microchannel with one branch heated is used for the study. Deremble and Tabeling [8] experimentally studied the droplet breakup process in microfluidic junction with arbitrary angles (Y-junction). Choi *et al.* [9] suggested a new method for producing asymmetrical droplets by using the pneumatic valve in the tube through which continuous fluid and droplets flows. Zhu *et al.* [10] studied both experimentally and numerically the controllable breakup of droplets and bubble by using the pneumatic valve. Bedram and Moosavi [11] numerically investigated the droplet breakup in asymmetric microfluidic T-junction, which consists of an inlet channel and two outlet channels with different width. Wu *et al.* [12] experimentally studied the asymmetrical breakup of bubbles in a microfluidic T-junction with divergence and convergence section. Bedram and Moosavi [13] numerically studied the droplets breakup in micro and nanoscale T-junctions using volume of fluid (VOF) method. Hoang *et al.* [14] numerically studied the droplet breakup dynamics in a three-dimensional T-junction microchannel. Bedram *et al.* [15] numerically investigated an efficient method for generating unequal sized droplets in microfluidic and nanofluidic systems using volume-of-fluid (VOF) method. In this method, the breakup of droplets occurs by using a valve in one branch of the T-junction. From this, it was observed that smaller droplet moves to the branch with the valve. Thippavathini and Moharana [16] numerically studied the flow of Taylor bubble in a microchannel in which an obstacle is present. The obstacle is used for creating turbulence due to which the heat transfer capacity increases.

In this work, a two-dimension numerical simulation is carried out using commercially available ANSYS Fluent® to study hydrodynamics of Taylor bubble breakup using a microchannel having a downstream T-junction divergence where an obstacle is placed. Through the upstream T-junction air and water enters to the microchannel. Air is considered as dispersed phase, and water is considered as the continuous phase. Initially the microchannel is filled with water and air enters to the water filled microchannel, due to which Taylor bubble is created at the T-junction. The bubble breakup into two discrete daughter bubble at the T-junction divergence due to the presence of an obstacle. The breakup may be of symmetrical or asymmetrical depending upon the position of the obstacle at the T-junction divergence.

2. METHODOLOGY

I. Problem formulation

In this study, a microchannel with an upstream T-junction and a downstream T-junction is used as shown schematically in Fig. 1(a). Air (dispersed phase) and water (continuous phase) enters to the microchannel through the two inlets at the upstream T-junction and the Taylor bubble is created at the T-junction. There is an obstacle placed at the downstream T-junction as shown in Fig. 1(b), which helps to break the Taylor bubbles into two discrete Taylor bubbles having equal or unequal lengths depending upon the position of the obstacle.
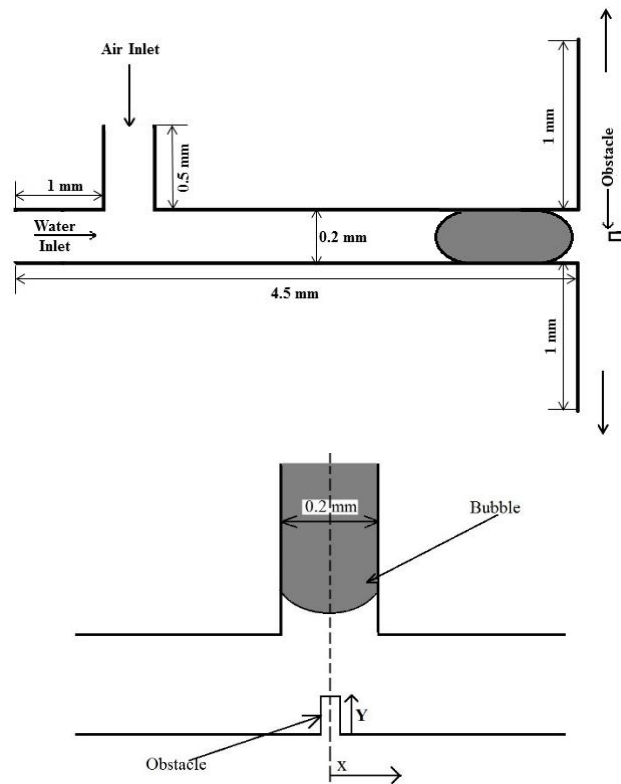
Fig. 1. (a) T-junction microchannel with a bifurcation, (b) Zoom view of the T-junction bifurcation with obstacle.

The microchannel having square cross-section with hydraulic diameter (D_h) of 0.2 mm and the length of the main channel is 4.5 mm. The obstacle width is 0.01 mm. By varying the position and height of the obstacle, different types of bubble breakup obtained such as symmetric breakup, asymmetric breakup and no breakup. The obstacle position ranged from the centre of the bifurcated T-junction to the right side branch (i.e. X = 0, 0.025, 0.05, 0.075 and 0.1 mm) and the height varied as (Y = 0.05, 0.1, 0.15 and 0.2

mm). Initially, the main channel was filled with water, and the side channel of the upstream T-junction with air. The air and water flow into the channel by assuming as laminar flow at the inlets. The water velocity at the inlet is set to 0.251 m/s according to the Re = 50 and the air velocity at the inlet is set to 0.154 m/s according to the Re = 2. Different cases are done by varying height and position of the obstacle. Some parameters like bubble length ratio, bubble breakup length, bubble breakup time and pressure drop at the time of bubble breakup are studied.
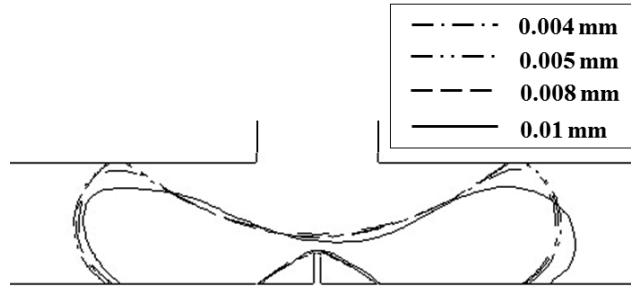
II. Grid independence test

Suitable grid size is selected based on grid independence test. In this work the grid independence test was carried out by taking four number of edge sizing, such as 0.01 mm, 0.008 mm, 0.005 mm and 0.004 mm. By using these edge sizing the grid generation occurs. After complete the solution, contours of the volume fraction of air just before the bubble breakup is captured for different edge sizing. Then the grid independence test result obtained by calculating the bubble length, as shown in Fig. 2.

From this, it is observed that for the grid size 0.01 mm, the shape and size of the bubble is not perfectly correct. For grid size 0.008 mm the bubble shape and size is better than that of for 0.01 grid size. However, for the grid size of 0.005 mm and 0.004 mm, the shape and size of the bubble is same and obtained a perfect shape. So for this problem the grid size of 0.005 mm was chosen. The grid size of 0.004 mm was not chosen because, for this grid size the number of elements is more which takes more time for simulation. So for consuming less time and for obtaining good results the grid size of 0.005 mm was taken.

III. Numerical analysis

The objective of this modeling of multiphase flow in the microchannel is to track the liquid-gas interface. For capturing the interface between liquid and gas, one of the fundamental multiphase models in ANSYS Fluent®, the Volume-of-Fluid (VOF) model is used. Iterative time advancement pressure based unsteady solver is used. The fluids taken for the study are water and air. Air is set as primary phase and water as the secondary phase. The fluid flow is considered as laminar at the inlet. Inlet velocity of water and air are set as 0.251 m/s and 0.154 m/s respectively. Pressure-outlet and no-slip were considered as the boundary condition for the outlet and wall respectively. PISO scheme was used for pressure-velocity coupling, Green-Gauss cell-based theorem used for gradient computation, for pressure discretization PRESTO scheme is used, the second order upwind scheme used for solving momentum equation. Variable time step is defined by taking global Courant number = 0.25, the ending time taken as 1000 s, the minimum and maximum time step size were considered as 10^{-8} and 10^{-4} respectively and all remaining values were set as default value. The number of time steps was set as 10^6 and maximum iteration/time step set as 20.

Fig. 2. Grid independence test result.

3. RESULTS AND DISCUSSION

The width of the obstacle was taken as 0.01 mm as shown in Fig. 1(b). The height of the obstacle (= Y) varied from 0.05 mm to 0.2 mm. The position of the obstacle varied from 0 to 0.1 mm, which is represented as X, its distance from the central position. Water and air enters to the microchannel through the inlets of upstream T-junction with a velocity of 0.251 m/s (Re = 50) and 0.154 m/s (Re = 2) respectively. After the formation of Taylor bubble at the upstream T-junction (which is not discussed here), the breakup process takes place at the downstream T-junction bifurcation. The objective of this study is to control the breakup process by varying the position and height of an obstacle at the T-junction bifurcation, which will result in different breakup process such as (i) symmetrical breakup (ii) asymmetrical breakup and (iii) no breakup. The symmetrical breakup of the Taylor bubble occurs when there is no obstacle is placed. This can be observed in Fig. 3. The bubble strikes at the T-junction bifurcation and then slowly grows at that location (see Fig. 3(ii)). After some time the breakup process of the bubble begins till both parts of the bubble snap from each other (see Fig. 3(iv) for the moment about to snap) and form two separate equal size bubble (see Fig. 3(vii)). This process, called symmetrical breakup will occur every time without any obstacle. The length of the breakup bubbles will depend on the length of the original bubble and the width/area of the bifurcated channel with respect to the original channel.
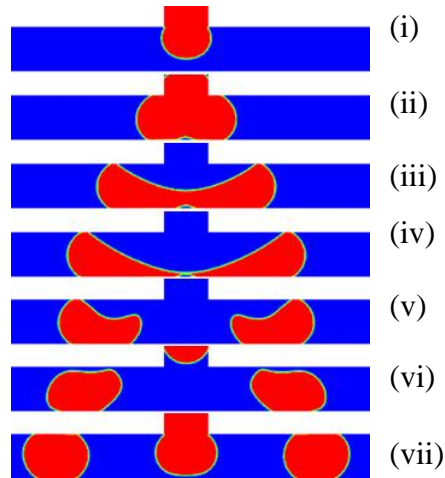
Fig. 3. The symmetrical breakup of the bubble at the T-junction bifurcation without any obstacle.
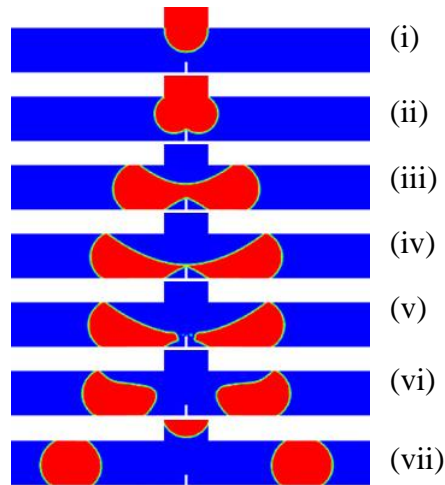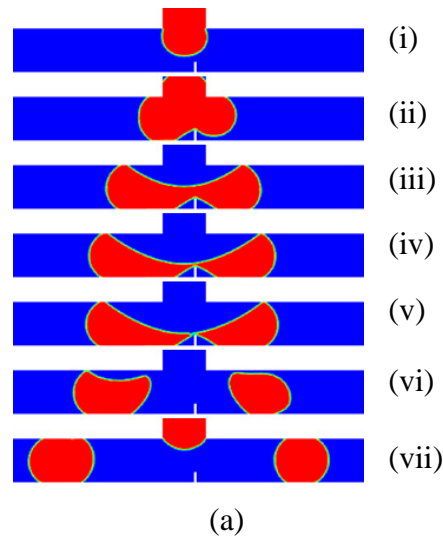

Fig. 4. The symmetrical breakup of the bubble when the obstacle is positioned at the center of the T-junction bifurcation.

Secondly, symmetrical breakup will occur when an obstacle is placed at the center of the T-junction bifurcation irrespective of the height of the obstacle (Y). Height of the obstacle does not influence the breakup process. This is because of equal spacing on both left and right side of the obstacle (towards the bifurcated channels) at any height. The breakup process for Y = 0.05 mm can be observed in Fig. 4. The tip of the bubble will first touch the tip of the obstacle, then the bubbles will start to grow on either side towards the bifurcated channel till the tail of the bubble touches the tip of the obstacle. Then the snapping of the bubbles from the tip of the obstacle will occur and the bubbles will try to regain their original shape. After travelling a small distance away from the obstacle, they will return to equilibrium position and regain

their original shape of Taylor bubble with reduced bubble length, as described earlier in previous paragraph. For the sake of brevity, the breakup process for different height of obstacle at the central position (X = 0) is not presented here.

Figure 5(a-c) presents asymmetrical breakup of Taylor bubble at the T-junction bifurcation due to presence of an obstacle at a distance of 0.05 mm (= X) away from the central position, for three different height of the obstacle, Y = 0.05, 0.1, and 0.15 mm respectively. For every case, the asymmetrical breakup occur because of unequal spacing on either side of the obstacle towards the bifurcated channels. Here because the obstacle is positioned towards the right of the central position, the spacing on the left of the obstacle is more than the spacing on the right of the obstacle. This is true for different height of the obstacle. Larger opening leads to lesser resistance; thus, longer will be the bubble length in the bifurcated channel, which is along the left branch, as shown in Fig. 5.

With increasing height of the obstacle, the opening on both side decreases. But, the ratio of opening on right to left of the obstacle decreases with increasing height of the obstacle. Because of this, the bubble length along the right side bifurcated branch goes on decreasing with increasing obstacle height. Therefore, the bubble length along the left side bifurcated branch goes on decreasing.


(a)

(b)

(c)
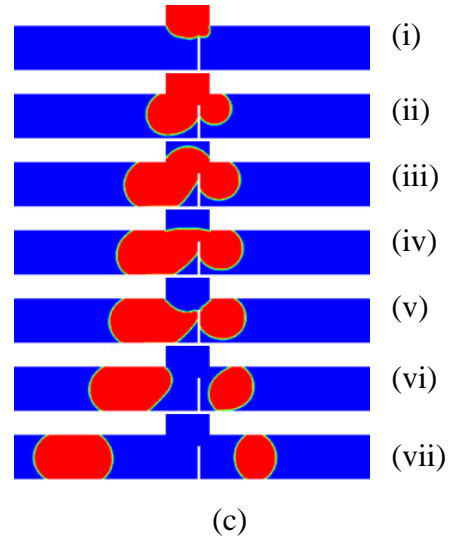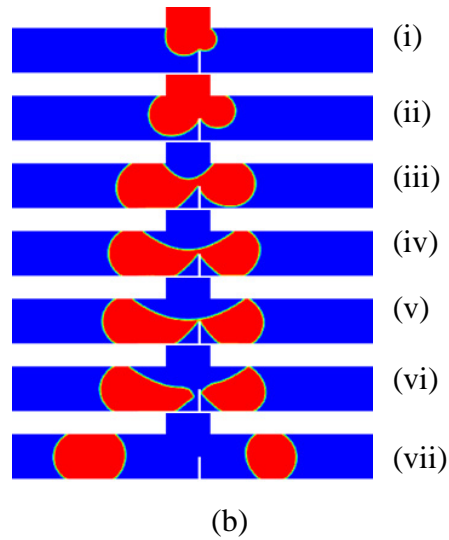
Fig. 5. The asymmetrical breakup of the bubble when the obstacle is positioned at 0.05 mm right to the center of the T-junction bifurcation for different height of the obstacle (a) 0.05 mm (b) 0.1 mm, and (c) 0.15 mm.

To explain the asymmetrical bifurcation in a more logical manner, two terms are defined; (i) bubble length ratio (ii) opening ratio. After the breakup of the parent Taylor bubble, two new daughter bubbles are formed and move into both the branches of the T-junction bifurcation. The length of these daughter bubbles will be less than that of the parent bubble. The bubble length ratio is defined as the ratio between the lengths of the bubble in right side branch to that of in left side branch (as shown in Fig. 6).
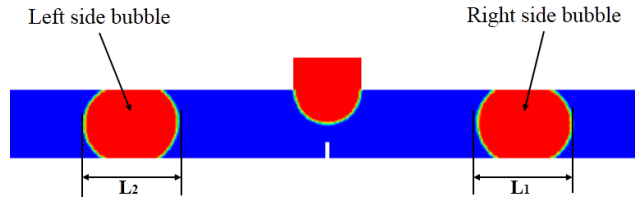
Fig. 6. Daughter bubbles in the bifurcated branches showing their lengths.

As discussed earlier, the opening width/area will be unequal on either side of the obstacle. Here the opening on left and the right side of the obstacle is represented by O_L and O_R respectively as shown in Fig. 7. The opening ratio is defined as the ratio of O_R to O_L.
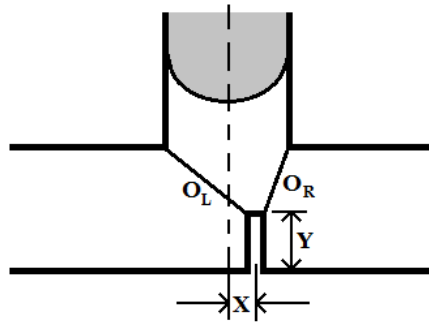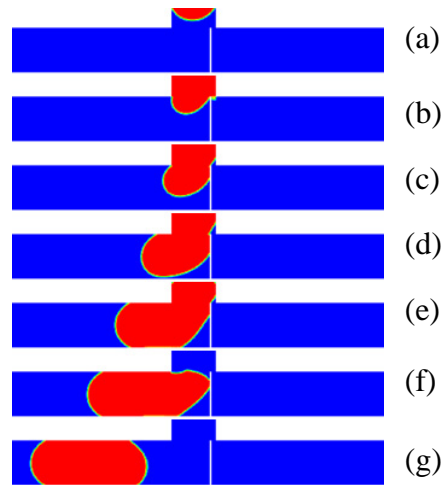

Fig. 7. T-junction bifurcation showing opening on either side of the obstacle.

Figure 8 shows variation of opening ratio and bubble length ratio with varying obstacle height when it is not positioned at the central location (at X = 0.05). Here it can be observed that both the curves are parallel to each other; indicating that increasing obstacle height causes decrease in opening ratio as well as bubble length ratio. This means, bubble length ratio is directly proportional to opening ratio, which is function of obstacle height. Thus, the bubble length ratio can be suitably controlled by changing the position and height of the obstacle.
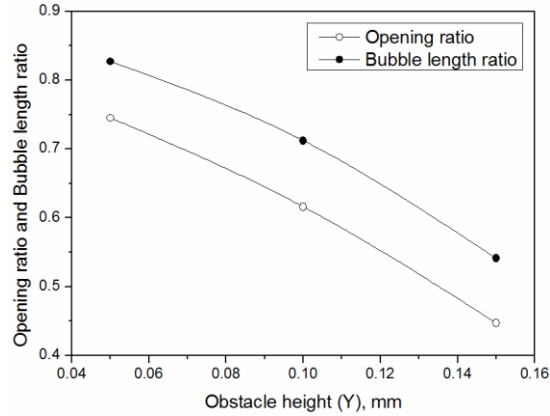
Fig. 8. Variation of opening ratio and bubble length ratio with varying obstacle height at X = 0.05 mm.

Fig. 9. Single bubble flow, when the obstacle positioned at 0.075 mm right to the center of the T-junction bifurcation and the height, is 0.2 mm.

When the opening on the right side of the obstacle O_R (see Fig. 7) decreases beyond some threshold value, the bubble will not be able to pass through this opening and will result in no bubble breakup. In such scenario, the bubble will pass through the left opening and will enter to the left bifurcated channel, as shown in Fig. 9. Figure 9 corresponds to obstacle position of X = 0.075 mm and obstacle height Y = 0.2 mm (which is equal to width of the bifurcated channels). This phenomena occur because of higher flow resistance across the right opening (O_R) compared to the left opening (O_L).

4. CONCLUSIONS

A two-dimensional numerical study of Taylor bubble breakup at T-junction bifurcation is carried out. An obstacle is positioned at the T-junction bifurcation to control the breakup of the Taylor bubble. By varying the position and height of the obstacle, the bubble size can be controlled as per need. It is found that the obstacle breaksup into two equal size (symmetrical breakup) when no obstacle is placed. Secondly, it is also observed that symmetrical break up of the bubble occur when the obstacle is placed at the central position irrespective of the height of the obstacle. When the obstacle is shifted from its central position, asymmetrical breakup of the Taylor bubble occur where both the position and height of the obstcale (or the opening ratio) decide the bubble length ratio. Finally, when the opening on one side of the obstacle decreases beyond some threshold value, the bubble will not be able to pass through this opening and will result in no bubble breakup.

REFERENCES

1. T. Thorsen, R. W. Roberts, F. H. Arnold, & S. R. Quake, (2001) Dynamic pattern formation in a vesicle-generating microfluidic device. Physical Review Letters, 86(18), 4163.

2. H. A. Stone, A. D. Stroock, & A. Ajdari, (2004) Engineering flows in small devices: microfluidics toward a lab-on-a-chip. Annual Review of Fluid Mechanics, 36, 381-411.

3. J. D. Tice, H. Song, A. D. Lyon, & R. F. Ismagilov, (2003) Formation of droplets and mixing in multiphase microfluidics at low values of the Reynolds and the capillary numbers. Langmuir, 19(22), 9127-9133.

4. D. R. Link, S. L. Anna, D. A. Weitz, & H. A. Stone, (2004) Geometrically mediated breakup of drops in microfluidic devices. Physical Review Letters, 92(5), 054503.

5. P. Garstecki, M. J. Fuerstman, H. A. Stone, & G. M. Whitesides, (2006) Formation of droplets and bubbles in a microfluidic T-junction-scaling and mechanism of break-up. Lab on a Chip, 6(3), 437-446.

6. Jousse, F., Farr, R., Link, D. R., Fuerstman, M. J., & Garstecki, P. (2006) Bifurcation of droplet flows within capillaries. Physical Review E, 74(3), 036311.

7. T. H. Ting, Y. F. Yap, N. T. Nguyen, T. N. Wong, Chai, J. C. K., & L. Yobas, (2006) Thermally mediated breakup of drops in microchannels. Applied Physics Letters, 89(23), 234101.

8. L. Ménétrier-Deremble, & P. Tabeling, (2006) Droplet breakup in microfluidic junctions of arbitrary angles. Physical Review E, 74(3), 035303.

9. Choi, J. H., Lee, S. K., Lim, J. M., Yang, S. M., & G. R. Yi, (2010) Designed pneumatic valve actuators for controlled droplet breakup and generation. Lab Chip, 10(4), 456-461.

10. H. W. Zhu, N. G. Zhang, R. X. He, S. Z. Li, S. S. Guo, W. Liu, & X. Z. Zhao, (2011) Controllable fission of droplets and bubbles by pneumatic valve. Microfluidics and Nanofluidics, 10(6), 1343-1349.

11. A. Bedram, & A. Moosavi, (2011) Droplet breakup in an asymmetric microfluidic T junction. The European Physical Journal E: Soft Matter and Biological Physics, 34(8), 1-8.

12. Y. Wu, T. Fu, C. Zhu, Y. Lu, Y. Ma, & H. Z. Li, (2012) Asymmetrical breakup of bubbles at a microfluidic T-junction divergence: feedback effect of bubble collision. Microfluidics and Nanofluidics, 13(5), 723-733.

13. A. Bedram, & A. Moosavi, (2012) Breakup of Droplets in Micro and Nanofluidic T-Junctions. Applied Mechanics and Materials, 110, 3673-3678.

14. D. A. Hoang, L. M. Portela, C. R. Kleijn, M. T. Kreutzer, & V. Van Steijn, (2013) Dynamics of droplet breakup in a T-junction. Journal of Fluid Mechanics, 717, R4.

15. A. Bedram, A. E. Darabi, A. Moosavi, & S. K. Hannani, (2015) Numerical Investigation of an Efficient Method (T-Junction with Valve) for Producing Unequal-Sized Droplets in Micro-and Nano-Fluidic Systems. Journal of Fluids Engineering, 137(3), 031202.

16. S. Thippavathini, & M. K. Moharana, (2014) Flow of Taylor bubble in microchannel having an obstacle. In ASME 2014 12th International Conference on Nanochannels, Microchannels, and Minichannels.

Nomenclature

C	Courant number
Re	Reynolds number
$\vec{F}$	Surface tension force of the liquid $(N/m^{2)})$
$\vec{v}$	Velocity vector (m/s)
u	Magnitude of velocity (m/s)
P	Pressure force $(N/m^{2)})$
D_h	Hydraulic diameter of the channel (mm)
X	Position of obstacle (mm)
Y	Height of obstacle (mm)
t	Time (s)

C_p Specific heat (J/kg-K)

k_f Thermal conductivity (W/m-K)

O_R Opening at the right side of the obstacle

O_L Opening at the left side of the obstacle

Greek symbol

ρ Density (kg/m^3)

μ Dynamic viscosity (N $-$s/m^2)

σ Coefficient of surface tension (N/m)

α Volume fraction

∇ Differential operator

Δt Time step size (s)

Δx Length interval (mm)

Subscript

L Liquid

G Gas

Superscript

T Transpose